

## Article

# A Comparative Probabilistic Seismic Hazard Analysis for Eastern Turkey (Bitlis) Based on Updated Hazard Map and Its Effect on Regular RC Structures

Ercan Işık <sup>1</sup>  and Ehsan Harirchian <sup>2,\*</sup> <sup>1</sup> Department of Civil Engineering, Bitlis Eren University, Bitlis 13100, Turkey<sup>2</sup> Institute of Structural Mechanics (ISM), Bauhaus-Universität Weimar, 99423 Weimar, Germany

\* Correspondence: ehsan.harirchian@uni-weimar.de

**Abstract:** Determining the earthquake hazard of any settlement is one of the primary studies for reducing earthquake damage. Therefore, earthquake hazard maps used for this purpose must be renewed over time. Turkey Earthquake Hazard Map has been used instead of Turkey Earthquake Zones Map since 2019. A probabilistic seismic hazard was performed by using these last two maps and different attenuation relationships for Bitlis Province (Eastern Turkey) were located in the Lake Van Basin, which has a high seismic risk. The earthquake parameters were determined by considering all districts and neighborhoods in the province. Probabilistic seismic hazard analyses were carried out for these settlements using seismic sources and four different attenuation relationships. The obtained values are compared with the design spectrum stated in the last two earthquake maps. Significant differences exist between the design spectrum obtained according to the different exceedance probabilities. In this study, adaptive pushover analyses of sample-reinforced concrete buildings were performed using the design ground motion level. Structural analyses were carried out using three different design spectra, as given in the last two seismic design codes and the mean spectrum obtained from attenuation relationships. Different design spectra significantly change the target displacements predicted for the performance levels of the buildings.

**Keywords:** Eastern Turkey; seismic risk; adaptive pushover; design spectra; Bitlis



**Citation:** Işık, E.; Harirchian, E. A Comparative Probabilistic Seismic Hazard Analysis for Eastern Turkey (Bitlis) Based on Updated Hazard Map and Its Effect on Regular RC Structures. *Buildings* **2022**, *12*, 1573. <https://doi.org/10.3390/buildings12101573>

Academic Editor: Marco Di Ludovico

Received: 2 September 2022

Accepted: 27 September 2022

Published: 30 September 2022

**Publisher's Note:** MDPI stays neutral with regard to jurisdictional claims in published maps and institutional affiliations.



**Copyright:** © 2022 by the authors. Licensee MDPI, Basel, Switzerland. This article is an open access article distributed under the terms and conditions of the Creative Commons Attribution (CC BY) license (<https://creativecommons.org/licenses/by/4.0/>).

## 1. Introduction

The main priority for reducing earthquake damage depends on the reliable determination of the seismic hazard. Risk is the combination of the probability or frequency of a defined threat and the magnitude of the consequences of the occurrence. In other words, the level of risk is proportional to the hazard's intensity (or magnitude) and the vulnerability of the affected elements [1,2]. After each earthquake, significant loss and damage to life and properties emphasize the necessity to demonstrate the seismic hazard reliably. Therefore, determining the seismic risk of any region is an integral part of modern pre-earthquake disaster management [3–7]. This is also important for the seismic sensitivity assessment and retrofit decision making of structures [8,9].

The assessment of seismic risk is recognized as an early and emerging new discipline that was introduced as a logical continuation of seismic hazard research that Luis Esteva (1967, 1968) [10,11] and Allin Cornell [12] carried out. As stated in an elementary definition of this discipline, outlined by the EERI Committee on Seismic Risk in 1984, “seismic risk is the probability that social and economic consequences of earthquakes will equal or exceed specified values at a site, at various sites or in an area during a specified exposure time” [13]. Opinions in the literature on initial earthquake risk assessment differ greatly. For example, Luis Esteva (1967, 1968) and Allin Cornell (1968) were the first to initiate seismic risk analysis in 1968. On the other hand, Whitman et al. pointed to several previous assessments of earthquake loss estimations, such as the NOAA1 study for San Francisco [14], and state

that earthquake loss studies follow this for more than thirty US regions [15]. On the other hand, long before these studies, John Freeman's Earthquake Damage and Earthquake Insurance [16], accepted as an earthquake damage prediction today, was published [17]. Afterwards, earthquake damage prediction was mostly regarded as part of the insurance sector until the publication of Cornell's work in 1968 [2]. After that, seismic hazard and risk analyses for different parts of the world were out using different methods, such as the Philippines [18], Bangladesh [19], Iran [20], Korean Peninsula [21], Pakistan [22,23], Croatia [5,24,25], Brazil [26], Italy [27], Argentina [28], Bosnia-Herzegovina [29], Malaysia and Singapore [30] and Turkey [31,32]. In addition, Turkey has smaller-scale studies for different provinces in the Eastern Anatolia region, such as Bingöl [33] and Van [34–36].

Seismicity is based on geological, tectonic and statistical data. Macro seismic data regarding the earthquake origin time, location, epicenter, source parameters and magnitude are the most important parameters in determining the seismic hazard of any region. Furthermore, the seismicity of a region is an indicator of a future earthquake in that region [37–39]. Therefore, the data from destructive earthquakes significantly contribute to determining seismic hazard zones more realistically and developing fundamental principles for the design of earthquake-resistant structures. Thus, Turkey's demand for renewal in seismic hazard maps and principles for designing earthquake-resistant structures, especially after the 2011 Van earthquakes, emerged. Thanks to the studies performed, both seismic hazard maps and seismic design codes were updated in 2018 and started to be used in 2019 [31,40–42].

In this study, Bitlis province was selected as it is located in Lake Van Basin in Eastern Turkey. Lake Van Basin is one of Turkey's current and intensive seismic activity regions. Specifically, the earthquakes, whose epicenter was Van province located in this basin, and the losses that come after the earthquakes have, once again, revealed the seismic risk of the basin. Figure 1 displays the districts of the Bitlis province and its geographical location.



**Figure 1.** Location of Bitlis and its districts.

Bitlis is a historical city surrounded by mountains, located on the strait passages connecting Eastern Anatolia to South-Eastern Anatolia, located between  $41^{\circ}33'–43^{\circ}$  and  $37^{\circ}54'–38^{\circ}58'$ . Bitlis is in a position worth examining due to the seismicity in Bitlis and especially its close surroundings and the earthquakes that occurred in the past. This study conducted a probabilistic seismic hazard analysis for Bitlis province, considering the seismic sources and attenuation relationships. The results are compared to the design spectra in the last two seismic design codes. In addition, structural analyses were performed by using the mean design spectrum obtained from the used attenuation relationships and the last two design spectra. The study is important regarding the site-specific seismic hazard analysis and comparing the last two earthquake hazard values for Bitlis. Furthermore,

different design spectra were tried to reveal at what level the earthquake hazard changes affect the building performance. Therefore, in light of current data and studies, the region's seismicity, the earthquake hazard and their behaviour under the effect of earthquakes should be reviewed.

## 2. Tectonics and Seismicity of Bitlis

It is a known fact that local geological soil conditions directly affect and alter seismic activity characteristics and may damage existing structures on these soils [43,44]. In the center of Bitlis and its vicinity, the metamorphic rocks of Bitlis massif, upper cretaceous mélangé in the Ahlat-Adilcevaz area, Eocene aged Ahlat conglomerate, Miocene aged Adilcevaz Limestone, polio-quadernary volcanism and alluvium outcrop are present. Rock assemblages are in the Van Lake Basin formed in the Paleozoic Era–present time period and alluvial sediment outcrop. Generally, the metamorphic rocks of the Bitlik Massif in are the south of the basin, volcanic and volcanoclastic rocks that are products of young Nemrut and Süphan are in the west and north areas, volcanic rocks and ophiolite components of the Yüksekova Complex are in the east of the basin, young-present streams and lacustrine sediments and carbonates outcrop [45–51]. The Bitlis Massif contains ophiolites of the old ocean floor and rock assemblages containing different metamorphic facies [52].

The Eastern Anatolia Region, located on the Alpine-Himalayan seismic belt, one of the most important seismic belts in the world, is seismically active. This area where these two faults in the nature of intra-continental transform faults limit the Anatolian plate and cross fault systems developed among them are a region with the highest density of active faults in Turkey. Eastern Anatolia is under continental shortening and thickening effects due to the continental collision between the Arabian and Eurasian plates [53–57]. In addition, the volcanism in the region was developed by this collision [49,58]. This active continental collision forces the Anatolian Plate to move counterclockwise to the west, along the North Anatolian Fault Zone (NAFZ) and East Anatolian Fault Zone (EAFZ), two major strike-slip fault zones (Figure 2) [59,60]. Sinistral-slip NAFZ and dextral-slip EAFZ join the Karliova Triple Junction (KTJ) located in Eastern Anatolia [61]. Many fault lines in Turkey have developed due to this active continental collision [59,62–66]. Both Bitlis-Zagros Suture Belt and Karliova Triple Junction are close to Bitlis province.

Lake Van, which is a product of the tectonic pressure led by the collision of the Arabian and Eurasian Plates [59,67,68] and partially remained in the province of Bitlis, is in a tectonic structure that has undergone intense deformation in Eastern Anatolia [69,70]. With its volume of 607 km<sup>3</sup> and a maximum depth of 451 m, Lake Van is the fourth largest lake in the world among inland lakes in terms of water content, after the Caspian Sea, the Aral Sea and Lake Issyk-Kul [71]. Therefore, earthquake activity is very high around Lake Van [72,73]. In addition, a major and destructive earthquake that may occur in the Lake Van Basin can closely affect the Bitlis city center and districts in this basin. Table 1 shows some major and destructive earthquakes around Bitlis in the instrumental period. The  $M \geq 5.0$  earthquakes in and around Bitlis between 1900 and 2017 are shown in Figure 3.

**Table 1.** Some significant earthquakes in and around Bitlis [78,79].

Date	Location	M	Earthquake Losses
1903	Malazgirt (Muş)	6.7	600 casualties and 450 building damage
1941	Van	5.9	192 casualties and 600 building damage
1946	Varto (Muş)	5.9	839 casualties and 3000 building damage
1949	Karliova(Bingöl)	6.7	450 casualties and 3500 building damage
1966	Varto (Muş)	6.9	2396 casualties and 20,007 building damage
1971	Bingöl	6.7	878 casualties and 9111 building damage
1975	Lice (Diyarbakır)	6.6	2385 casualties and 8149 building damage
1976	Muradiye (Van)	7.5	3840 casualties and 9232 building damage
2003	Bingöl	6.4	176 casualties and 6000 building damage
2004	Ağrı	5.1	17 casualties and 1000 building damage
2011	Tabanlı (Van)	7.2	644 casualties and 17,005 building damage
2011	Edremit (Van)	5.6	40 casualties

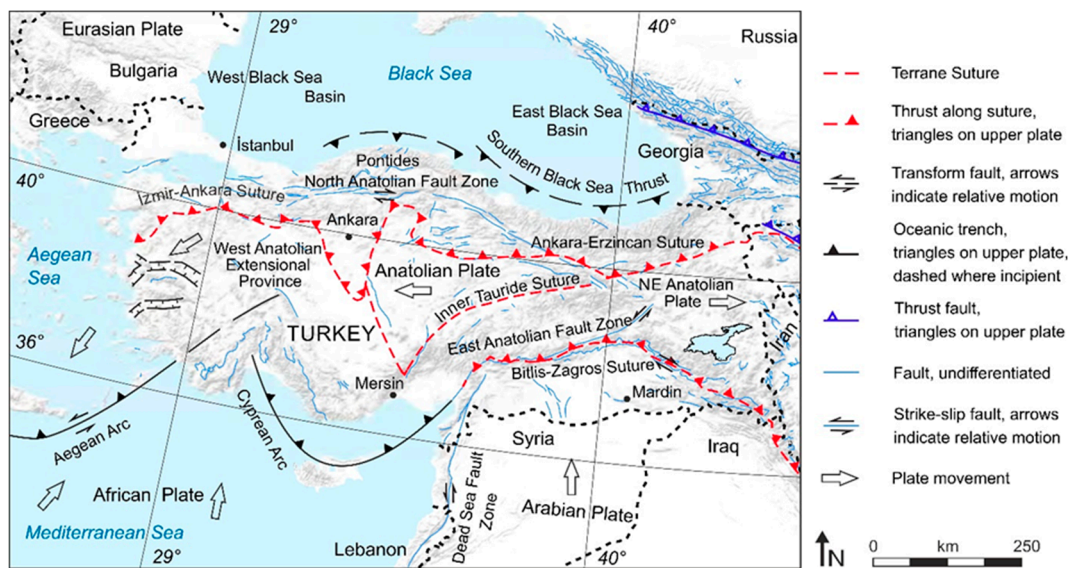


Figure 2. Simplified neotectonic map of Turkey and the surroundings [74–77].

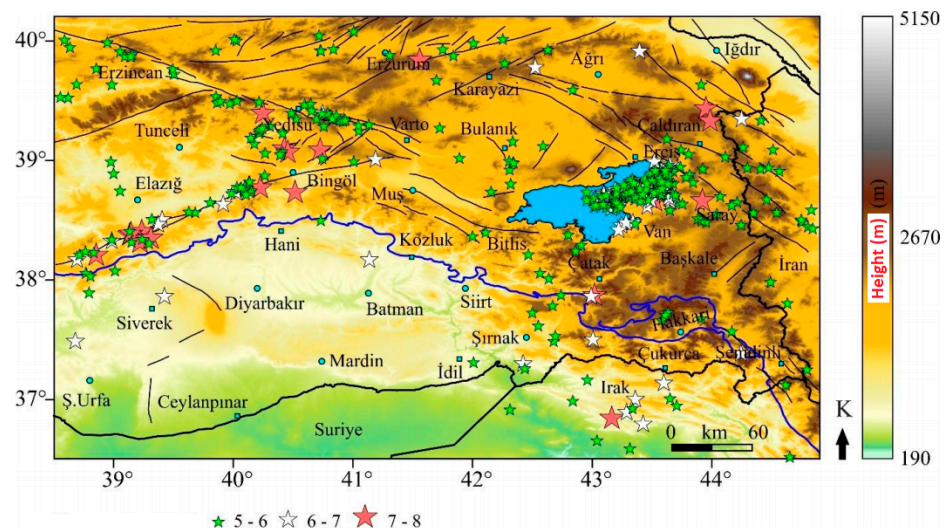


Figure 3.  $M \geq 5.0$  earthquakes surroundings Bitlis between 1900 and 2017 [80].

### 3. Current Seismic Parameters of Bitlis

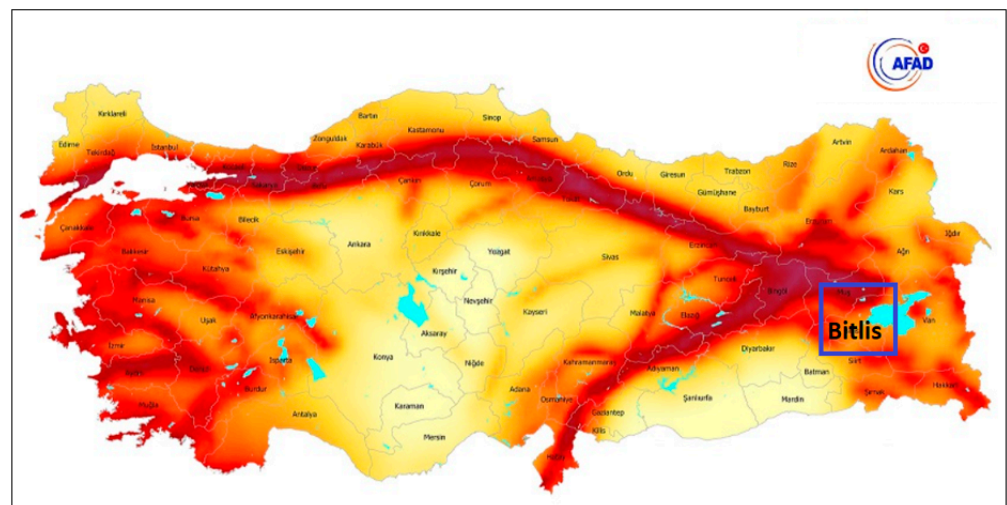
The fact that December 27, 1939, Erzincan, December 20, 1942, Niksar–Erbaa, June 20, 1943, Adapazari–Hendek, November 26, 1943, Tosya–Ladik and February 1, 1944, Bolu–Gerde earthquakes occurred at close time intervals and led to huge economic losses and casualties triggered the efforts to reduce earthquake losses in Turkey [81,82]. Turkey’s first official earthquake zonation map was prepared in 1945 following these earthquakes [83,84]. The historical development in these maps is shown in Table 2.

Table 2. The published official maps of earthquake zones in Turkey.

Year	Name	Method
1945	Map of earthquake zones	Based on damage data
1947	Map of earthquake zones	Based on damage data
1963	Turkey Earthquake Zones Map	Based on deterministic approach
1972	Turkey Earthquake Zones Map	Based on deterministic approach
1996	Turkey Earthquake Zones Map	Based on probabilistic approach
2018	Turkish Earthquake Hazard Map	Based on probabilistic approach

In the seismic hazard models used in the creation of the earthquake hazard map published in 1996, the errors resulting from the use of the attenuation relationship obtained from Western US measurements were ignored due to lack of data in the earthquake catalogue, uncertainties in the geographical boundaries of earthquake source faults and lack of local data [85]. The Seismic Zoning Map of Turkey, which entered into force in 1996, was renewed by the Disaster & Emergency Management Authority, Presidential of Earthquake Department and published in 2018 and became effective as of January 1, 2019. The new map was prepared in cooperation with the public and universities through the project titled Updating Turkey Earthquake Hazard Maps, which was supported by the AFAD National Earthquake Research Programme (UDAP). The new map was prepared with much more detailed data, considering the most up-to-date earthquake source parameters, earthquake catalogues and next-generation mathematical models. Unlike the previous map, the new map includes peak ground acceleration values rather than earthquake zones and the concept was removed [86–88].

In the studies of determining the source zone forming the basis for creating the earthquake hazard map that entered into force in 2019, a total of 105 seismic sources was identified by taking into account the active fault database of Turkey [89] and the earthquake catalogue [90]. The highest earthquake magnitudes of these seismic sources were determined after statistical analysis of instrumental and historical earthquake catalogues. In addition, the ground motion databases of Turkey, Greece, Italy, and California, which have similar seismotectonic structures, were compiled, and a broad, strong ground motion database was created. Moreover, four ground motion prediction equations that best represent this database were used in probabilistic seismic hazard analysis with a different emphasis [91]. An updated earthquake hazard map of Turkey is given in Figure 4.



**Figure 4.** Updated Turkish Earthquake Hazard Map.

Turkish Earthquake Hazard Maps have started to be used with the Turkish Building Earthquake Code (TBEC-2018). Thanks to these maps, earthquake and earthquake-building parameters of any geographical location can be determined. These values can be obtained practically using the Turkey Earthquake Hazard Maps Interactive Web Application (TEHMIWA). Ground motion levels for four different exceedance probabilities were identified in the TBEC-2018 (Table 3).

The peak ground acceleration (PGA) and peak ground velocity (PGV) obtained for different probabilities of exceedance of all neighborhoods in Bitlis province are shown in Table 4.

**Table 3.** Earthquake ground motion levels [40].

Earthquake Level	Repetition Period (Year)	Probability of Exceedance (in 50 Years)	Description
DD-1	2475	2%	Largest earthquake ground motion
DD-2	475	10%	Standard design earthquake ground motion
DD-3	72	50%	Frequent earthquake ground motion
DD-4	43	68%	Service earthquake movement

**Table 4.** PGA and PGV values for all neighbourhoods in the city center of Bitlis.

Neighbourhood	Peak Ground Acceleration (g)				Peak Ground Velocity (cm/s)-PGV			
	Probability of Exceedance in 50 Years				Probability of Exceedance in 50 Years			
	2%	10%	50%	68%	2%	10%	50%	68%
Atatürk	0.490	0.260	0.107	0.077	28.306	15.149	6.547	4.878
Beş Minare	0.493	0.261	0.107	0.078	28.503	15.276	6.620	4.936
Gazi Bey	0.490	0.260	0.106	0.077	28.249	15.104	6.525	4.861
Hersan	0.489	0.260	0.106	0.076	28.132	15.016	6.475	4.821
Hüsrev Paşa	0.491	0.260	0.107	0.077	28.403	15.211	6.585	4.909
İnönü	0.490	0.260	0.106	0.077	28.213	15.078	6.509	4.848
Muştababa	0.490	0.260	0.106	0.077	28.214	15.080	6.505	4.843
Saray	0.490	0.260	0.106	0.077	28.176	15.050	6.487	4.828
Sekiz Ağustos	0.490	0.259	0.106	0.077	28.148	15.025	6.484	4.830
Şemsi Bitlis	0.490	0.260	0.106	0.077	28.197	15.066	6.501	4.841
Taş	0.490	0.260	0.107	0.077	28.308	15.153	6.545	4.874
Yükseliş	0.491	0.261	0.107	0.077	28.397	15.222	6.573	4.892
Zeydan	0.490	0.260	0.106	0.077	28.260	15.116	6.523	4.856

There are seven districts (Adilcevaz, Ahlat, Güroymak, Hizan, Mutki and Tatvan) in Bitlis province, including the central district. The southern side of the Nemrut volcanic mount in the province of Bitlis is located 10 km from the Tatvan district and about 24 km from Bitlis central district. Mount Süphan, which is approximately 85 km away from Bitlis city center and part of which is located within the boundaries of Adilcevaz district, is the highest mountain of volcanic origin (4058 m) in Turkey after the Mount of Greater Agri (Ararat). Table 5 compares PGA and PGV values measured by different earthquake ground motion levels for seven districts of Bitlis province.

**Table 5.** PGA and PGV values for different probabilities of exceedance for Bitlis districts.

District	Peak Ground Acceleration (g)-PGA				Peak Ground Velocity (cm/s)-PGV			
	Probability of Exceedance in 50 Years				Probability of Exceedance in 50 Years			
	2%	10%	50%	68%	2%	10%	50%	68%
Adilcevaz	0.578	0.303	0.121	0.086	37.108	18.625	7.399	5.345
Ahlat	1.038	0.570	0.203	0.128	62.602	32.921	11.090	7.075
Güroymak	0.549	0.296	0.118	0.085	32.817	17.744	7.485	5.405
Hizan	0.522	0.281	0.110	0.078	28.693	14.955	6.239	4.588
Merkez	0.490	0.260	0.106	0.078	28.193	15.063	6.500	4.841
Mutki	0.522	0.280	0.109	0.078	30.507	16.212	6.770	4.964
Tatvan	0.502	0.265	0.109	0.079	29.017	15.512	6.731	5.042

Turkish Earthquake Hazard Map Interactive Web Application (TEHMIWA) has become available for the computation of earthquake parameters used in structural analyses for any geographic location since the beginning of 2019 [86,88]. The seismic hazard maps obtained for Bitlis and its districts for the earthquake ground motion level (DD-1) that is a 2% probability of exceedance (repetition period 2475 years) in 50 years is given in

Figure 5A, for 10% is given in Figure 5B, for 50% is given in Figure 5C and for 68% is given in Figure 5D by using TEHMIWA.

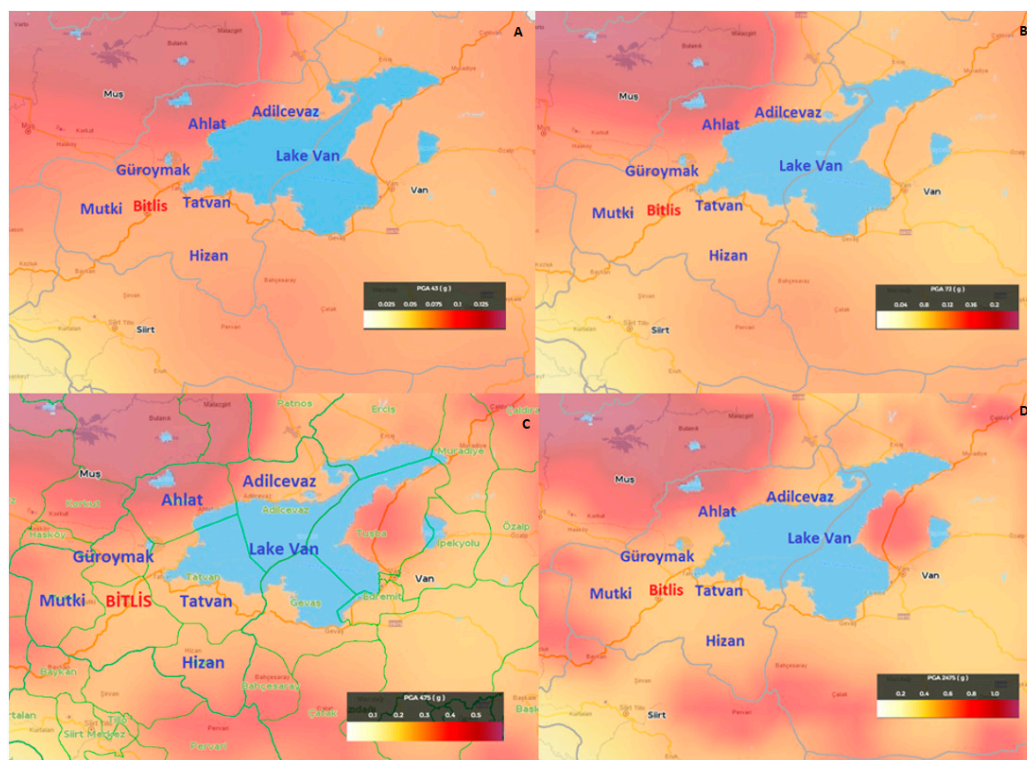


Figure 5. Seismic hazard maps for different probabilities of exceedance; (A) 2%, (B) 10%, (C) 50%, (D) 68%.

In order to make comparisons for design spectra, the ZB class was chosen as the local ground condition from the local soil class given in TBEC-2018. The features of this soil class are given in Table 6.

Table 6. Local soil class type ZB [40].

Local Soil Class	Soil Type	Upper Average at 30 m		
		$(V_s)_{30}$ [m/s]	$(N60)_{30}$ [Pulse/30 cm]	$(cu)_{30}$ [kPa]
ZB	Slightly weathered, medium tough rocks	760–1500	—	—

Figures 6 and 7 compare horizontal and vertical elastic design spectra obtained when the DD-2 ground motion level of Bitlis districts and local soil profile belongs to the ZB soil type. The vertical elastic design spectrum first started to be used with TBEC-2018.

According to TSDC-2007 and TBEC-2018, the spectral acceleration coefficients and dominant ground periods of the design earthquake (DD-2) with a 10% probability of exceedance in 50 years are shown in Table 7. DD-2 ground motion level was chosen because it is included in the last two seismic design codes.

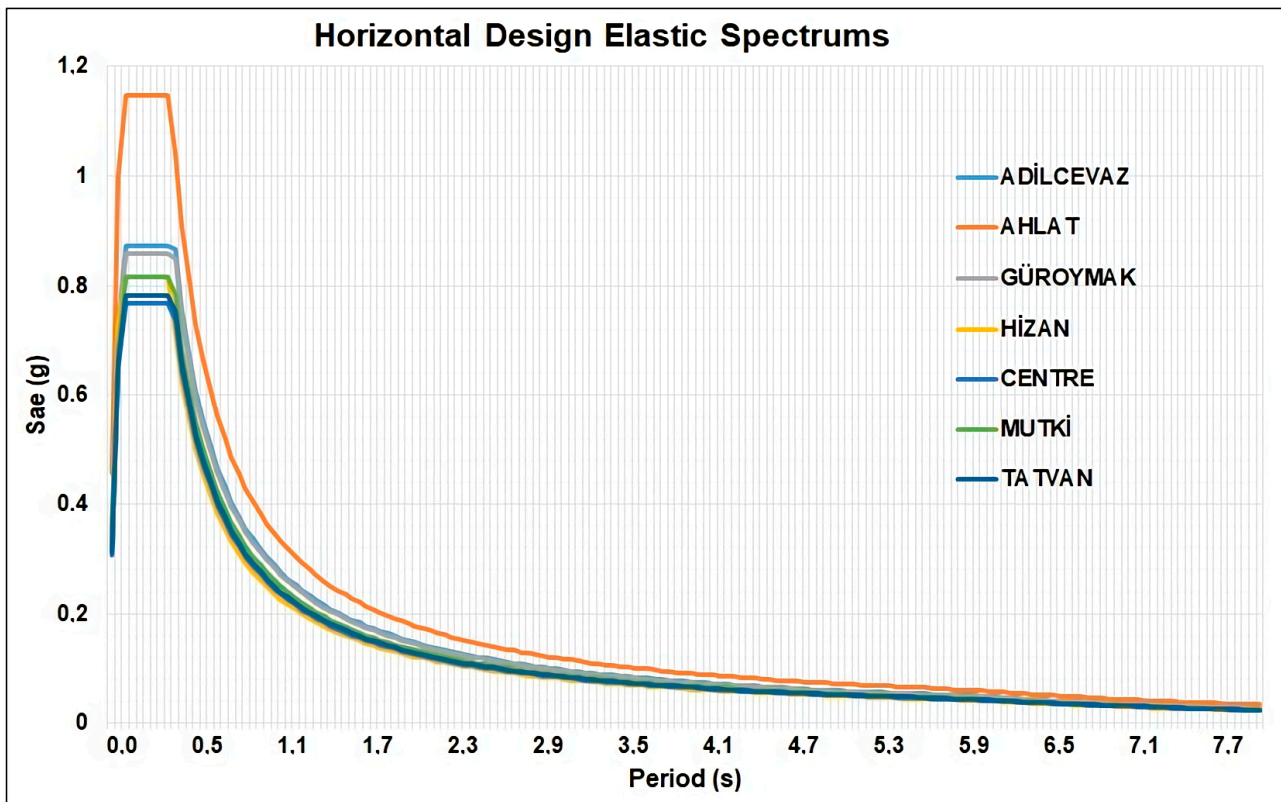


Figure 6. Comparison of horizontal elastic design spectra (DD-2/ZB).

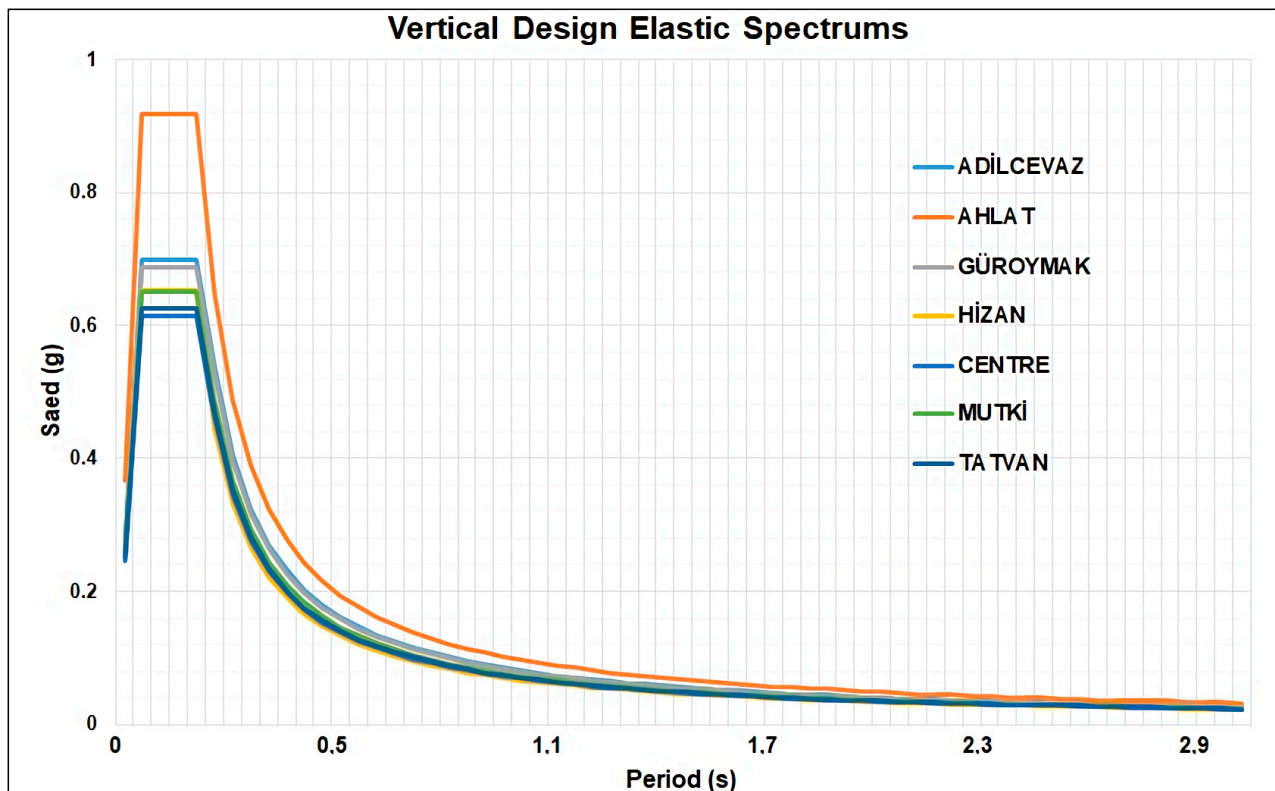


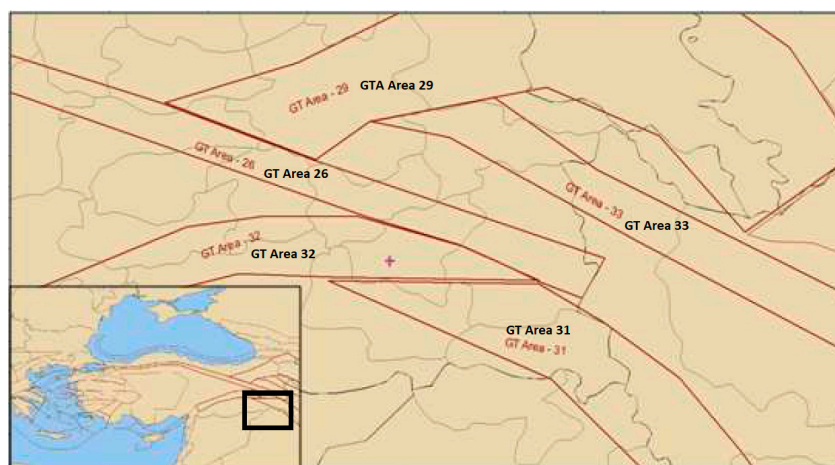
Figure 7. Comparison of vertical elastic design spectra (DD-2/ZB).

**Table 7.** The comparison of spectral acceleration coefficients with ground type ZB.

DD-2 District	Spectral Acceleration Coefficients All Ground Types				Horizontal				Vertical			
	TSDC-2007		TBEC-2018		ZB		ZB		ZB		ZB	
	$S_{DS}$	$0.40S_{DS}$	$S_{DS}$	$0.40S_{DS}$	$T_A$	$T_B$	$T_A$	$T_B$	$T_{AD}$	$T_{BD}$	$T_{AD}$	$T_{BD}$
Adilcevaz	1	0.4	0.638	0.255	0.15	0.40	0.050	0.249	There is no vertical spectrum curve in this code	0.017	0.083	
Ahlat	1	0.4	1.227	0.491	0.15	0.40	0.043	0.214		0.014	0.071	
Güroymak	0.75	0.3	0.634	0.254	0.15	0.40	0.050	0.250		0.017	0.083	
Hizan	1	0.4	0.597	0.239	0.15	0.40	0.045	0.223		0.015	0.074	
Merkez	1	0.4	0.552	0.221	0.15	0.40	0.050	0.249		0.017	0.083	
Mutki	1	0.4	0.593	0.237	0.15	0.40	0.049	0.247		0.016	0.082	
Tatvan	0.75	0.3	0.559	0.224	0.15	0.40	0.050	0.249		0.017	0.083	

#### 4. Seismic Hazard Analyses

The threat posed by earthquakes on human activities in many parts of the world is a sufficient reason for carefully considering earthquakes in design structures and facilities. Seismic hazard analysis is the first step in earthquake risk assessment. Seismic hazard analysis involves quantitatively estimating ground-shaking hazards in a particular area. The main purpose of the seismic hazard analysis is to measure the parameters related to seismic ground motion (acceleration, velocity, displacement) for calculating the seismic loading conditions that the ground and engineering structures will be exposed to in the future [92,93]. In this study, Probabilistic Seismic Hazard Analysis (PSHA) for Bitlis city center was made using EZ-FRISK v7.43 software developed by Robin McGuire. In the calculations, two data sets were used to select earthquake sources. First, a study was conducted by considering regional data in the EZ-FRISK program database valid for Greece, Turkey, Lebanon, Syria and Israel. In this context, the areal earthquake sources of GT Area 26 (North Anatolian Fault), GT Area 31 (Bitlis Thrust Belt-East), GT Area 32 (Bitlis Thrust Belt-West) and GT Area 33 (Van-North) were taken into account in the analysis (Figure 8). Secondly, Bitlis's fault groups and surroundings were defined as areal sources. Since there are many fault and fault groups in the region and the fault parameters cannot be defined, the necessity of defining areal sources as earthquake sources has emerged. The study defined fault groups as Kavakbaşı, Bitlis Thrust-North, Bitlis Thrust, Van East, Suphan, Ahlat, and Malazgirt zones (Figure 9).

**Figure 8.** Areal earthquake sources in the database of EZ-FRISK software for Bitlis.

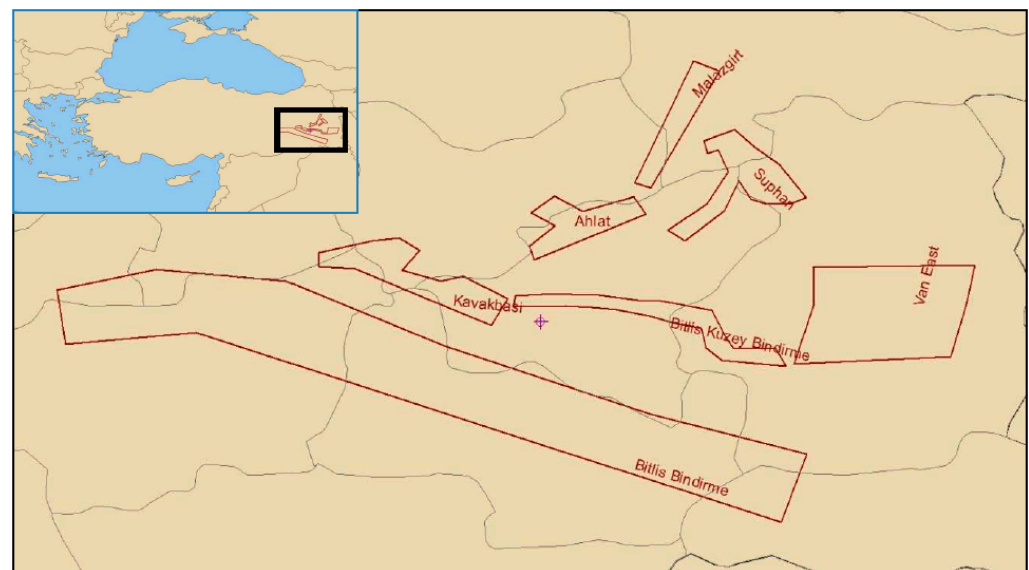


**Figure 9.** Definition of fault groups as areal earthquake source in Bitlis and its vicinity.

These areal earthquake sources are used to measure the change in spectral accelerations at periods for the earthquakes with a 50%, 10% and 2% probability of exceedance in 50 years. The strong ground motion acceleration records for the Eastern Anatolia region are very limited. The Abrahamson-Silva (1997) [94] and Campbell (2003) NGA Ground-Motion Relations [95], which is valid for shallow earthquakes around the world, the Graizer-Kalkan (2009) [96], which is valid in active tectonic zones around the world and Idriss (2008) [97] attenuation relations, which is developed for strike-slip shallow earthquakes, were used in the study. The software program obtained peak ground acceleration values as a function of the return periods. Uniform probability response spectra were obtained for the selected return periods. Figure 10 shows the response spectra for the Ahlat district with the highest risk of earthquake hazard, which has a 50% probability of exceedance in 50 years and a 72-year return period. A comparison of response spectra with a probability of exceedance in 50 years and a recurrence period of 475 years for Ahlat is shown in Figure 11.

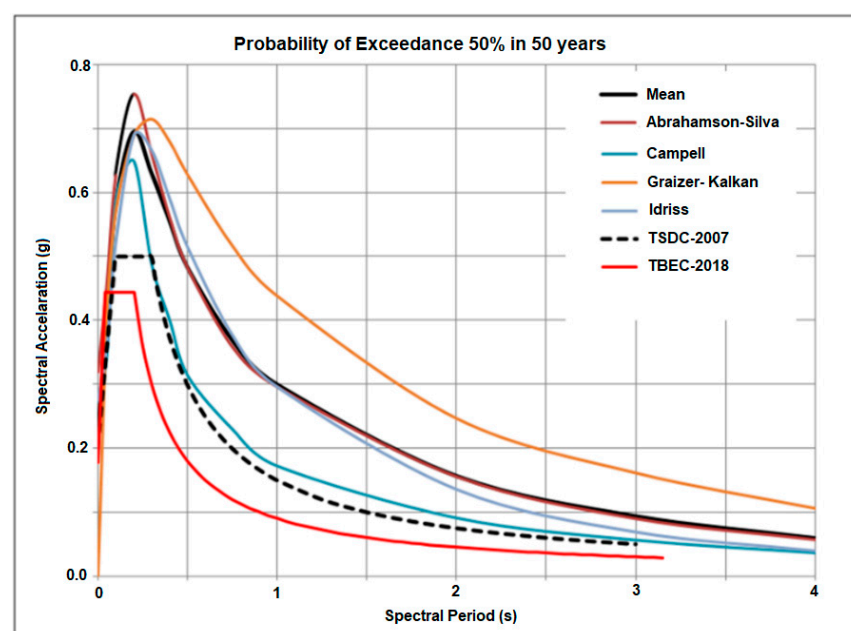


**Figure 10.** Comparison of response spectra with a return period of 72 years for Ahlat district.

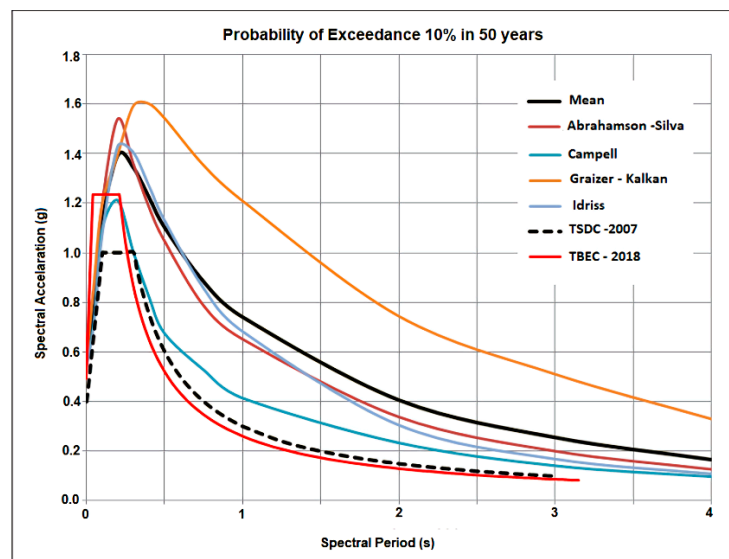


**Figure 11.** Comparison of response spectra with a return period of 475 years for Ahlat district.

A comparison of response spectra with a probability of exceedance in 50 years and a recurrence period of 2475 years for Ahlat is shown in Figure 12.

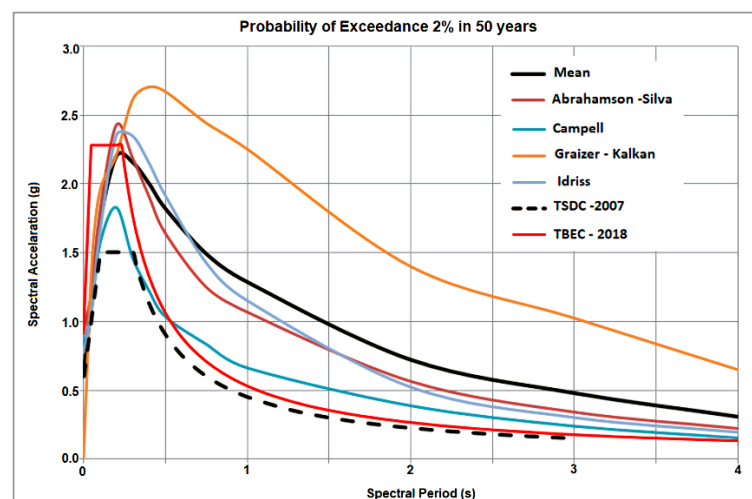


**Figure 12.** Comparison of response spectra with a return period of 2475 years for Ahlat district.

## 5. Structural Analysis

Structural analyses were carried out using academic licensed Seismostruct software.

Static pushover analysis has been widely used to determine the seismic behavior of structures. Various pushover analysis methods have been developed, including modal pushover, adaptive pushover, and cyclic pushover, where some of the weaknesses of the traditional pushover method are eliminated [98]. In this study, the static adaptive pushover analysis method was used. In this method, the effect of the frequency content and deformation of the ground motion on the structure's dynamic behavior is considered to determine the structure's capacity under horizontal loads. Furthermore, in this method, analysis was carried out taking into account the mode shapes and participation factors obtained from the eigenvalue analyses performed at each step. As a result, load distributions and strain profiles can be obtained for the structure with the help of the method. In conventional pushover analysis, the input functionality and load control types are similar to static adaptive pushover analysis [99–105]. This procedure can be expressed under four main headings: (i) definition of nominal load vector and inertia mass, (ii) computation of load

factor, (iii) calculation of normalized scaling vector, and (iv) update of loading displacement vector [106]. The flow chart of the adaptive pushover analyses is given in Figure 13.

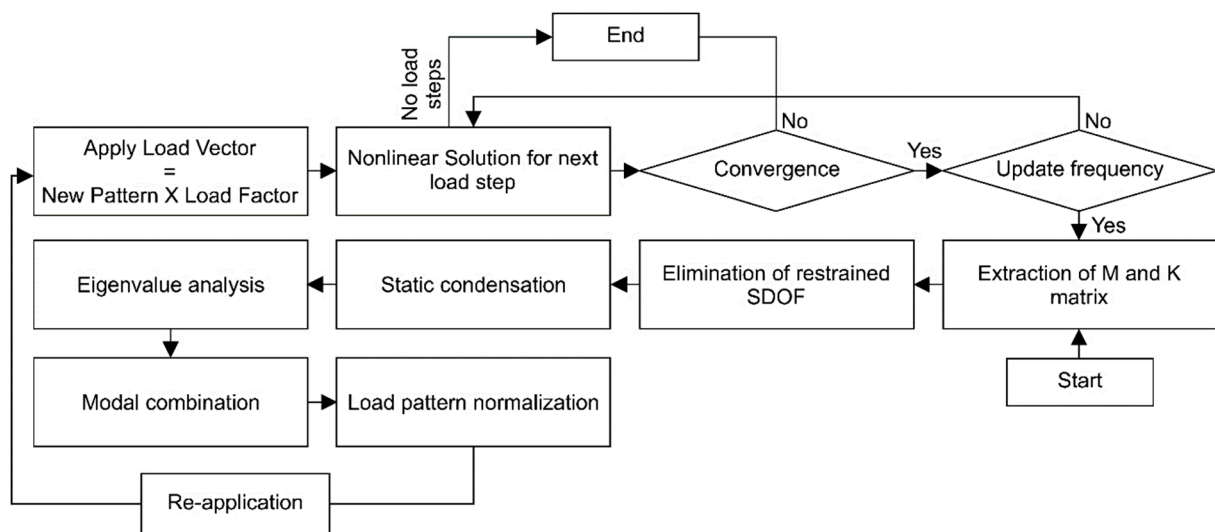


**Figure 13.** Flow chart of the adaptive pushover method (modified from [107]).

A seven-story RC building with the same structural characteristics was chosen as an example to reveal the structural analysis result differences for the settlements on the same fault zone. The analyses were performed in only one direction, since the RC building was chosen symmetrically in both directions. Five equal spans of 5 m length are considered in both the X and Y directions. A seven-story RC building with a total length of 2500 cm in both X and Y directions was chosen as the structural model. The blueprint of the selected RC building is given in Figure 14.

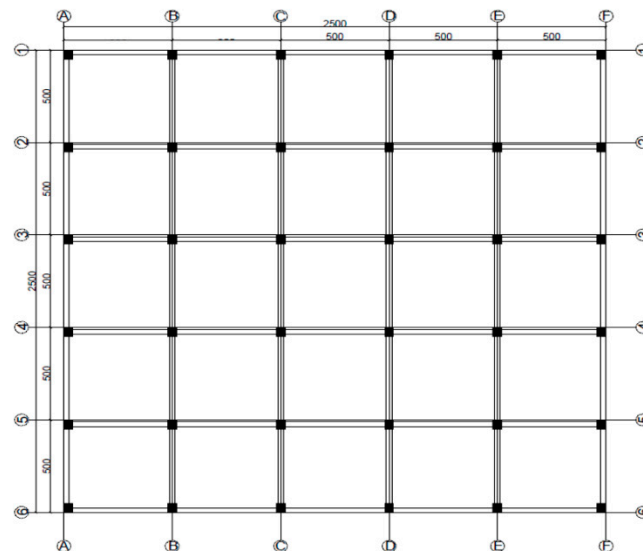


**Figure 14.** The blueprint of sample RC building.

Permanent and incremental loads were applied to the structure of the software. Incremental load values were selected as displacement. Permanent load values of 5.00 kN were taken into consideration. The target displacement was selected as 0.42 m. All these values were the same in all structural models used in this study. The three-dimensional model obtained in the software for the structure and the loads that were applied are given in Figure 14. The Menegotto-Pinto steel model (stl\_mp) for all reinforcement in structural

elements and Mander et al. nonlinear concrete model (con\_ma) for concrete were selected as material model.

Each story had an equal height and was taken as 3 m. The material class used for all load-bearing elements of the structure was selected as C25-S420. All columns were selected as  $0.40 \times 0.50$  m and beams were selected as  $0.25 \times 0.60$  m. The transverse reinforcements used in both elements were selected as  $\phi 10/10$ . The reinforcements used in the columns were selected as  $4\phi 20$  at the corners and  $4\phi 16$  on the top, bottom and left–right sides. The reinforcements used in the beams were selected as  $4\phi 16$  on the lower side,  $5\phi 14$  on the upper side and  $2\phi 12$  on the side. The damping ratio was taken as % 5 in all structural models. The ZB class was chosen as the ground class. The importance of structure was taken into consideration in Class II. The slabs were selected as rigid diaphragms. The 2D and 3D structural models are shown in Figure 15.

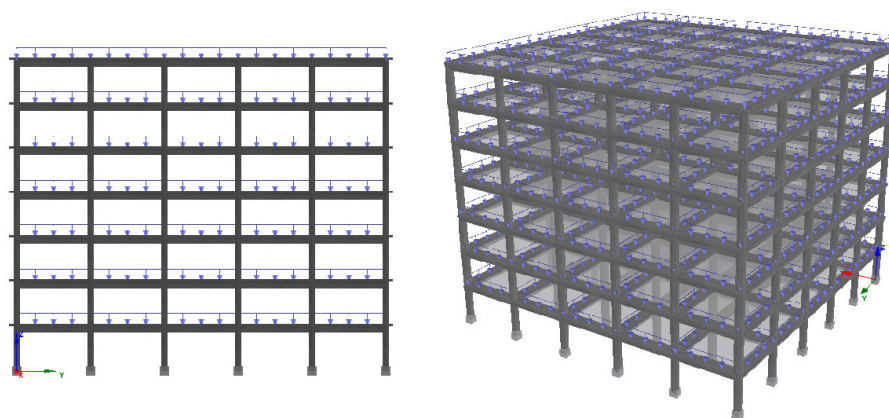


Figure 15. 2D and 3D models of the sample RC building.

Structural characteristics taken into account while creating the sample reinforced concrete building model are shown in Table 8.

Table 8. The structural characteristics of sample RC building.

Parameter	Value	
Concrete grade	C25	
Reinforcement grade	S420	
Story height	3.0 m	
Beams	$250 \times 600$ mm	
Height of floor	120 mm	
Cover thickness	25 mm	
Columns	$400 \times 500$ mm	
Longitudinal Reinforcement	Corners	$4\phi 20$
	Top bottom side	$4\phi 16$
	Left right side	$4\phi 16$
Transverse reinforcement	$\phi 10/100$	
Steel material Model	Menegotto-Pinto steel model (stl_mp)	
Concrete material model	Mander et al. nonlinear concrete model (con_ma)	
Constraint type	Rigid diaphragm	
Permanent Load	5 kN/m	
Target Displacement	0.42 m	
Ground Type	ZB	
Importance Class	II	
Damping ratio	5%	

The force-based plastic-hinged frame members (infrmFBPH) are selected for structural elements in the sample RC building model. These elements model the spread inelasticity

based on force and only limit the plasticity to a finite length. In total, 100 fiber elements are defined for the selected sections. This value is sufficient for such sections. Plastic-hinge length ( $L_p/L$ ) was chosen as 16.67%.

The sample RC building was analyzed using the three different horizontal design spectrum curves, such as mean, TSDC-2007 and TBEC-2018, obtained for Ahlat. As a result of the analysis, the base shear forces were calculated for each spectrum. The displacement values were obtained for three different points on the idealized curve. The first value refers to displacement at the moment of yield, the second value refers to the intermediate ( $d_{int}$ ) displacement and the third value refers to the target displacement. Elastic stiffness ( $K_{elas}$ ) and effective stiffness ( $K_{eff}$ ) values were calculated separately for all models. Three different performance criteria were obtained for damage estimation. These are considered as near collapse (NC), significant damage (SD) and damage limitation (DL). All these values are calculated separately for different design spectra. The comparison of all values obtained in the X direction as a result of structural analyses is shown in Table 9.

**Table 9.** Comparison of the result values obtained for X direction.

Spectrum Type	Base Shear (kN)	Displacement (m)	$K_{elas}$ (kN/m)	$K_{eff}$ (kN/m)	DL (m)	SD (m)	NC (m)
Mean	8981.73	0.1019	202,200.17	88,118.27	0.2162	0.2773	0.4807
		0.2091					
		0.4181					
TSDC-2007	8973.51	0.1039	202,200.17	88,065.00	0.1018	0.1304	0.2263
		0.2098					
		0.4191					
TBEC-2018	8980.65	0.1021	202,200.17	87,944.03	0.1468	0.1884	0.3226
		0.2093					
		0.4182					

The stiffness value of any structural reinforced-concrete element differs from the estimated stiffness value under the impact of earthquake. Therefore, the concept of effective cross-sectional stiffness has emerged in the analysis and design of RC structural members. The stiffness of the cracked sections of RC structural systems is taken into account to determine its performance under earthquake loads. The effective stiffness of the cracked sections is obtained using the predicted stiffness reduction coefficients of the elastic stiffness value [108–110]. In this study, elastic stiffness ( $K_{elas}$ ) and effective stiffness ( $K_{eff}$ ) values were directly obtained by using the stiffness reduction coefficients estimated in the software used.

## 6. Conclusions

During the update of earthquake hazard maps in 2018, the province of Bitlis and its districts located in the Eastern Anatolia Region were considered a region with a high earthquake risk in Turkey. PGA and PGV values were obtained for different probabilities of exceedance. According to the values obtained within the scope of this study, PGA values in 50 years for the province were found as follows: 0.49–1.04 g for 2% probability of exceedance; 0.26–0.57 g for 10% probability of exceedance; 0.010–0.20 g for 50% probability of exceedance; and 0.08–0.13 g for 68% probability of exceedance, respectively. The study obtained horizontal and vertical elastic design spectra for each district by choosing the same local soil class. The order of magnitude of PGA values has also remained valid for design spectrum. Computation of design spectrum on a point basis indicates that the earthquake behaviour of structures can be calculated more realistically.

This study is important regarding the joint implementation of the Turkey Building Earthquake Code that entered into force in 2019 and the Turkey Earthquake Hazard Maps presented with this code. Changes were observed in the result values obtained for all neighborhoods and districts in Bitlis province. It was concluded that the reason for these differences is due to factors, such as site-specific seismicity characteristics, fault groups and their characteristics, the distance of the selected geographical locations to the fault/fault

groups and earthquake history of the region. The results indicate that obtaining design spectra by considering the site-specific earthquake hazard stipulated in the new earthquake code is remarkable. Furthermore, earthquake data will give applicable and practical results thanks to the transition from macro-zoning to micro-zoning.

Since the structural properties were kept constant in the sample RC building model considered in all settlements, the base shear force, elastic and effective stiffness values and period values were approximately equal. However, the differentiation in the design spectrum significantly changed the target displacements predicted for the expected performance levels of the structure. This reveals once again that the design spectrum significantly affects the target displacements expected from the buildings and, thus, the building performance level under impact of earthquake. While the greatest displacement values were obtained for the design spectrum obtained by considering the average of the attenuation relations, the lowest values were obtained using the design spectrum stipulated in the previous code. By comparing the stipulated values in the last two codes, it is concluded that the requests for displacement requests in the last regulation were greater.

**Author Contributions:** Conceptualization, E.I. and E.H.; methodology, E.I. and E.H.; software, E.I.; validation, E.I. and E.H.; formal analysis, E.H.; investigation E.I.; resources, E.I.; data curation, E.I. and E.H., writing—original draft preparation, E.I. and E.H.; writing—review and editing, E.H. and E.I.; visualization, E.H.; supervision, E.H. and E.I.; project administration, E.I.; funding acquisition, E.H. All authors have read and agreed to the published version of the manuscript.

**Funding:** This research received no external funding.

**Institutional Review Board Statement:** Not applicable.

**Informed Consent Statement:** Not applicable.

**Data Availability Statement:** Most data are included in the manuscript.

**Acknowledgments:** We acknowledge the support of the German Research Foundation (DFG) and the Bau-haus-Universität Weimar within the Open-Access Publishing Programme.

**Conflicts of Interest:** The authors declare no conflict of interest.

## References

1. Okuyama, Y.; Chang, S.E. *Modeling Spatial and Economic Impacts of Disasters*; Springer Science & Business Media: Berlin, Germany, 2004.
2. Coburn, A.; Spence, R. *Earthquake Protection*, 2nd ed.; John Wiley & Sons: Chichester, UK, 2002.
3. Isik, E.; Isik, M.F.; Bulbul, M.A. Web based evaluation of earthquake damages for reinforced concrete buildings. *Earthq. Struct.* **2017**, *13*, 387–396.
4. Strukar, K.; Sipos, T.K.; Jelec, M.; Hadzima-Nyarko, M. Efficient damage assessment for selected earthquake records based on spectral matching. *Earthq. Struct.* **2019**, *17*, 271–282.
5. Pavić, G.; Hadzima-Nyarko, M.; Bulajić, B. A contribution to a UHS-based seismic risk assessment in Croatia—A Case Study for the City of Osijek. *Sustainability* **2020**, *12*, 1796. [[CrossRef](#)]
6. Büyüksaraç, A.; Işık, E.; Bektaş, Ö. A comparative evaluation of earthquake code change on seismic parameter and structural analysis; a case of Turkey. *Arab. J. Sci. Eng.* **2022**, 1–21. [[CrossRef](#)]
7. Avcil, F.; Işık, E.; Bilgin, H.; Özmen, H.B. Tbdy-2018'de verilen tasarım spektrumlarının anıtsal yapı sismik davranışına etkisi. *Adıyaman Üniversitesi Mühendislik Bilim. Derg.* **2022**, *9*, 165–177.
8. Shabani, A.; Alinejad, A.; Teymouri, M.; Costa, A.N.; Shabani, M.; Kioumars, M. Seismic vulnerability assessment and strengthening of heritage timber buildings: A review. *Buildings* **2021**, *11*, 661. [[CrossRef](#)]
9. Xu, M.; Zhang, P.; Cui, C.; Zhao, J. An ontology-based holistic and probabilistic framework for seismic risk assessment of buildings. *Buildings* **2022**, *12*, 1391. [[CrossRef](#)]
10. Esteva, L. Criterios para la construcción de espectros para diseño sísmico. In Proceedings of the XII Jornadas Sudamericanas de Ingeniería Estructural y III Simposio Panamericano de Estructuras, Caracas, Venezuela, 2–8 July 1967; Boletín del Instituto de Materiales y Modelos Estructurales, Universidad Central de Venezuela: Caracas, Venezuela, 1967.
11. Esteva, L. Bases Para la Formulación de Decisiones de Diseño Sísmico. Ph.D. Thesis, Universidad Autónoma Nacional de México, Mexico City, Mexico, 1968.
12. Cornell, C.A. Engineering seismic risk analysis. *Bull. Seismol. Soc. Am.* **1968**, *58*, 1583–1606. [[CrossRef](#)]

13. Lang, D. Earthquake Damage and Loss Assessment—Predicting the Unpredictable. Ph.D. Thesis, University of Bergen, Bergen, Norway, 2012.
14. Algermissen, S.T.; Rinehart, W.A.; Dewey, J.; Steinbrugge, K.V.; Degenkolb, H.J.; Cluff, L.S.; McClure, F.E.; Gordon, R.F.; Scott, S.; Lagorio, H.J. *A Study of Earthquake Losses in the San Francisco Bay Area: Data and Analysis*; Office of Emergency Preparedness and National Oceanic and Atmospheric Administration: Washington, DC, USA, 1972.
15. National Institute of Building Sciences. *Assessment of State-of-the-Art Earthquake Loss Estimation Methodologies, FEMA249*; Federal Emergency Management Agency: Washington, DC, USA, 1994.
16. Freeman, J.R. *Earthquake Damage and Earthquake Insurance: Studies of a Rational Basis for Earthquake Insurance, also Studies of Engineering Data for Earthquake Resisting Construction*; McGraw-Hill Book Co.: New York, NY, USA, 1932.
17. Kircher, C.A.; Reitherman, R.K.; Whitman, R.V.; Arnold, C. Estimation of earthquake losses to buildings. *Earthq. Spectra* **1997**, *13*, 703–720. [[CrossRef](#)]
18. Peñarubia, H.C.; Johnson, K.L.; Styron, R.H.; Bacolcol, T.C.; Sevilla, W.I.G.; Perez, J.S.; Bonita, J.D.; Narag, I.C.; Solidum, R.U., Jr.; Pagani, M.M.; et al. Probabilistic seismic hazard analysis model for the Philippines. *Earthq. Spectra* **2020**, *36*, 44–68. [[CrossRef](#)]
19. Rahman, M.Z.; Siddiqua, S.; Kamal, A.M. Seismic source modeling and probabilistic seismic hazard analysis for Bangladesh. *Nat. Hazards* **2020**, *103*, 2489–2532. [[CrossRef](#)]
20. Mahsuli, M.; Rahimi, H.; Bakhshi, A. Probabilistic seismic hazard analysis of Iran using reliability methods. *Bull. Earthq. Eng.* **2019**, *17*, 1117–1143. [[CrossRef](#)]
21. Alam, J.; Kim, D.; Choi, B. Seismic probabilistic risk assessment of weir structures considering the earthquake hazard in the Korean Peninsula. *Earthq. Struct.* **2017**, *13*, 421–427.
22. Khan, S.; Waseem, M.; Khan, M.A.; Ahmed, W. Updated earthquake catalogue for seismic hazard analysis in Pakistan. *J. Seismol.* **2018**, *22*, 841–861. [[CrossRef](#)]
23. Abid, M.; Isleem, H.F.; Shahzada, K.; Khan, A.U.; Kamal Shah, M.; Saeed, S.; Aslam, F. Seismic hazard assessment of Shigo Kas Hydro-Power Project (Khyber Pakhtunkhwa, Pakistan). *Buildings* **2021**, *11*, 349. [[CrossRef](#)]
24. Šipoš, T.K.; Hadzima-Nyarko, M. Seismic risk of Croatian cities based on building’s vulnerability. *Tehnički Vjesnik* **2018**, *25*, 1088–1094.
25. Hadzima-Nyarko, M.; Kalman Sipos, T. Insights from existing earthquake loss assessment research in Croatia. *Earthq. Struct.* **2017**, *13*, 365–375.
26. Almeida, A.A.D.; Assumpção, M.; Bommer, J.J.; Drouet, S.; Riccomini, C.; Prates, C.L. Probabilistic seismic hazard analysis for a nuclear power plant site in southeast Brazil. *J. Seismol.* **2019**, *23*, 1–23. [[CrossRef](#)]
27. Ebrahimian, H.; Jalayer, F.; Forte, G.; Convertito, V.; Licata, V.; d’Onofrio, A.; Santo, A.; Silvestri, F.; Manfredi, G. Site-specific probabilistic seismic hazard analysis for the western area of Naples, Italy. *Bull. Earthq. Eng.* **2019**, *17*, 4743–4796. [[CrossRef](#)]
28. Gregori, S.D.; Christiansen, R. Seismic hazard analysis for central-western Argentina. *Geod. Geodyn.* **2018**, *9*, 25–33. [[CrossRef](#)]
29. Ademović, N.; Hadzima-Nyarko, M.; Zagora, N. Seismic vulnerability assessment of masonry buildings in Banja Luka and Sarajevo (Bosnia and Herzegovina) using the macroseismic model. *Bull. Earthq. Eng.* **2020**, *18*, 3897–3933. [[CrossRef](#)]
30. Looi, D.T.; Tsang, H.H.; Hee, M.C.; Lam, N.T. Seismic hazard and response spectrum modelling for Malaysia and Singapore. *Earthq. Struct.* **2018**, *15*, 67–79.
31. Akkar, S.; Kale, Ö.; Yakut, A.; Ceken, U. Ground-motion characterization for the probabilistic seismic hazard assessment in Turkey. *Bull. Earthq. Eng.* **2018**, *16*, 3439–3463. [[CrossRef](#)]
32. Nas, M.; Lyubushin, A.; Softa, M.; Bayrak, Y. Comparative PGA-driven probabilistic seismic hazard assessment (PSHA) of Turkey with a Bayesian perspective. *J. Seismol.* **2020**, *24*, 1109–1129. [[CrossRef](#)]
33. Balun, B.; Nemutlu, O.F.; Benli, A.; Sari, A. Estimation of probabilistic hazard for Bingol province, Turkey. *Earthq. Struct.* **2020**, *18*, 223–231.
34. Kutanis, M.; Ulutaş, H.; Işık, E. PSHA of Van province for performance assessment using spectrally matched strong ground motion records. *J. Earth Syst. Sci.* **2018**, *127*, 99. [[CrossRef](#)]
35. Büyüksaraç, A.; Işık, E.; Harirchian, E. A case study for determination of seismic risk priorities in Van (Eastern Turkey). *Earthq. Struct.* **2021**, *20*, 445–455.
36. Selcuk, L.; Selcuk, A.S.; Beyaz, T. Probabilistic seismic hazard assessment for Lake Van basin, Turkey. *Nat. Hazards* **2010**, *54*, 949–965. [[CrossRef](#)]
37. Kramer, S.L. Seismic hazard analysis. In *Geotechnical Earthquake Engineering*; Springer Science & Business Media: Berlin, Germany, 1996; pp. 106–142.
38. Ozmen, B.; Can, H. Deterministic seismic hazard assessment for Ankara, Turkey. *J. Fac. Eng. Arch. Gazi Uni.* **2016**, *31*, 9–18.
39. Işık, E. Comparative investigation of seismic and structural parameters of earthquakes ( $M \geq 6$ ) after 1900 in Turkey. *Arab. J. Geosci.* **2022**, *15*, 971. [[CrossRef](#)]
40. TBEC-2018, *Turkish Building Earthquake Code, T.C. Resmi Gazete*; Disaster and Emergency Management Presidency of Turkey: Ankara, Turkey, 2018.
41. AFAD. 2021. Available online: <https://tdth.afad.gov.tr> (accessed on 15 November 2021).
42. Çeken, U.; Dalyan, İ.; Kılıç, N.; Köksal, T.S.; Tekin, B.M. Türkiye Deprem Tehlike Haritaları İnteraktif Web Uygulaması. 4. In Proceedings of the International Earthquake Engineering and Seismology Conference, Bucharest, Romania, 14–17 June 2017.

43. Borchardt, R.D. A theoretical model for site coefficients in building code provisions. In Proceedings of the 13th World Conference on Earthquake Engineering, Vancouver, BC, Canada, 1–6 August 2004; pp. 1–6.
44. Işık, E.; Büyüksaraç, A.; Aydın, M.C. Effects of local soil conditions on earthquake damages. In *Journal of Current Construction Issues. Civil Engineering Present Problems, Innovative Solutions—Sustainable Development in Construction*; Görecki, J., Ed.; BGJ Consulting: Bydgoszcz, Poland, 2016; pp. 191–198.
45. Ketin, İ. Van Gölü ile İran sınırı arasındaki bölgede yapılan jeoloji gözlemlerinin sonuçları hakkında kısa bir açıklama. *Türkiye Jeol. Kurumu Bülteni* **1977**, *20*, 79–85.
46. Ternek, Z. Van Gölü Güney Doğu Bölgesinin jeolojisi. *Türkiye Jeol. Bülteni* **1953**, *4*, 1–32.
47. Goncuoglu, M.C.; Turhan, N. Geology of the Bitlis metamorphic belt. In *Geology of the Taurus Belt. International Symposium*; MTA: Ankara, Turkey, 1984; pp. 237–244.
48. Helvacı, C.; Griffin, W.L. *Rb-Sr Geochronology of the Bitlis Massif, Avnik (Bingöl) Area, SE Turkey*; Special Publications, Geological Society: London, UK, 1984; Volume 17, pp. 403–413.
49. Yılmaz, Y.; Güner, Y.; Şaroğlu, F. Geology of the Quaternary volcanic centres of the East Anatolia. *J. Volcanol. Geotherm. Res.* **1998**, *85*, 173–210. [[CrossRef](#)]
50. Ustaömer, P.A.; Ustaömer, T.; Collins, A.S.; Robertson, A.H. Cadomian (Ediacaran–Cambrian) arc magmatism in the Bitlis Massif, SE Turkey: Magmatism along the developing northern margin of Gondwana. *Tectonophysics* **2009**, *473*, 99–112. [[CrossRef](#)]
51. Işık, E. Seismic Performance Analysis of Bitlis City. Ph.D. Thesis, Institute of Natural Science, Sakarya University, Sakarya, Turkey, 2010.
52. Yılmaz, Y.; Dilek, Y.; Işık, H. Gevaş (Van) ofiyolitinin jeolojisi ve sinkinematik bir makaslama zonu. *Türkiye Jeol. Kurumu Bülteni* **1981**, *24*, 37–45.
53. Şengör, A.M.C.; Kidd, W.S.F. Post-collisional tectonics of the Turkish-Iranian plateau and a comparison with Tibet. *Tectonophysics* **1979**, *55*, 361–376. [[CrossRef](#)]
54. Şengör, A.M.C.; Yılmaz, Y. Tethyan evolution of Turkey: A plate tectonic approach. *Tectonophysics* **1981**, *75*, 181–241. [[CrossRef](#)]
55. Dewey, J.F.; Hempton, M.R.; Kidd, W.S.F.; Saroglu, F.A.; Şengör, A.M.C. *Shortening of Continental Lithosphere: The Neotectonics of Eastern Anatolia—A Young Collision Zone*; Special Publications, Geological Society: London, UK, 1986; Volume 19, pp. 1–36.
56. Utkucu, M.; Durmuş, H.; Yalçın, H.; Budakoglu, E.; Isik, E. Coulomb static stress changes before and after the 23 October 2011 Van, eastern Turkey, earthquake (MW = 7.1): Implications for the earthquake hazard mitigation. *Nat. Hazards Earth Syst. Sci.* **2013**, *13*, 1889. [[CrossRef](#)]
57. Alkan, H.; Büyüksaraç, A.; Bektaş, Ö.; Işık, E. Coulomb stress change before and after 24.01. 2020 Sivrice (Elazığ) Earthquake (Mw = 6.8) on the East Anatolian Fault Zone. *Arab. J. Geosci.* **2021**, *14*, 2648. [[CrossRef](#)]
58. Koçyiğit, A.; Yılmaz, A.; Adamia, S.; Kuloshvili, S. Neotectonics of East Anatolian Plateau (Turkey) and Lesser Caucasus: Implication for transition from thrusting to strike-slip faulting. *Geodin. Acta* **2001**, *14*, 177–195. [[CrossRef](#)]
59. McKenzie, D. Active tectonics of the Mediterranean region. *Geophys. J. Int.* **1972**, *30*, 109–185. [[CrossRef](#)]
60. Burke, K.; Şengör, A.M.C. Tectonic Escape in the Evolution of the Continental Crust. In *Reflection Seismology: The Continental Crust*; Barazangi, M., Brown, L., Eds.; American Geophysical Union: Washington, DC, USA, 1986; pp. 41–53.
61. Gök, R.; Mahdi, H.; Al-Shukri, H.; Rodgers, A.J. Crustal structure of Iraq from receiver functions and surface wave dispersion: Implications for understanding the deformation history of the Arabian–Eurasian collision. *Geophys. J. Int.* **2008**, *172*, 1179–1187. [[CrossRef](#)]
62. Ketin, İ. Über die tektonisch-mechanischen Folgerungen aus den großen anadoluischen Erdbeben des letzten Dezenniums. *Geol. Rundsch.* **1948**, *36*, 77–83. [[CrossRef](#)]
63. Dewey, J.F.; Şengör, A.M.C. Aegean and surrounding regions: Complex multiplate and continuum tectonics in a convergent zone. *Geol. Soc. Am. Bull.* **1979**, *90*, 84–92. [[CrossRef](#)]
64. Turkelli, N.; Sandvol, E.; Zor, E.; Gok, R.; Bekler, T.; Al-Lazki, A.; Barazangi, M. Seismogenic zones in eastern Turkey. *Geophys. Res. Lett.* **2003**, *30*. [[CrossRef](#)]
65. Horasan, G.; Boztepe-Güney, A. Observation and analysis of low-frequency crustal earthquakes in Lake Van and its vicinity, eastern Turkey. *J. Seismol.* **2007**, *11*, 1–13. [[CrossRef](#)]
66. Ateş, Y.; Yakupoğlu, T. Assessment of lacustrine/fluviat clays as liners for waste disposal (Lake Van Basin, Turkey). *Environ. Earth Sci.* **2012**, *67*, 653–663. [[CrossRef](#)]
67. Öztürk, B.; Balkıs, N.; Güven, K.C.; Aksu, A.; Görgün, M.; Ünlü, S.; Hanilci, N. Investigations on the sediment of Lake Van, II. heavy metals, sulfur, hydrogen sulfide and thiosulfuric acid S-(2-amino ethyl ester) contents. *J. Black Sea/Medit. Environ.* **2005**, *11*, 125–138.
68. Utkucu, M. 23 October 2011 Van, Eastern Anatolia, earthquake (M w 7.1) and seismotectonics of Lake Van area. *J. Seismol.* **2013**, *17*, 783–805. [[CrossRef](#)]
69. Işık, E. Bitlis ili'nin depremselliği. *Erciyes Üniversitesi Bilim. Enstitüsü Bilim. Dergisi* **2013**, *29*, 267–273.
70. Utkucu, M.; Budakoğlu, E.; Yalçın, H.; Durmuş, H.; Gülen, L.; Işık, E. Seismotectonic characteristics of the 23 October 2011 Van (Eastern Anatolia) earthquake (Mw = 7.1). *Bull. Earth Sci. Appl. Res. Cent. Hacet. Univ.* **2014**, *35*, 141–168.
71. Degens, E.T.; Wong, H.K.; Kempe, S.; Kurtman, F.J.G.R. A geological study of Lake Van, eastern Turkey. *Geol. Rundsch.* **1985**, *73*, 701–734. [[CrossRef](#)]

72. Toker, M.; Krastel, S.; Demirel-Schlueter, F.; Demirbağ, E.; Imren, C. Volcano-seismicity of Lake Van (Eastern Turkey), a comparative analysis of seismic reflection and three component velocity seismogram data and new insights into volcanic lake seismicity. In Proceedings of the International Earthquake Symposium, Kocaeli, Turkey, 22–26 October 2007; pp. 103–109.
73. Toker, M.; Sengor, A.C.; Schluter, F.D.; Demirbağ, E.; Cukur, D.; Imren, C. The structural elements and tectonics of the Lake Van basin (Eastern Anatolia) from multi-channel seismic reflection profiles. *J. Afr. Earth Sci.* **2017**, *129*, 165–178. [CrossRef]
74. Okay, A.I.; Tüysüz, O. *Tethyan Sutures of Northern Turkey*; Special Publications, Geological Society: London, UK, 1999; Volume 156, pp. 475–515.
75. USGS. *Porphyry Copper Assessment of the Tethys Region of Western and Southern Asia*; Scientific Investigations Report 2010-5090-V; U.S. Geological Survey: Reston, VA, USA, 2010.
76. Ekinci, Y.L.; Yiğitbaş, E. Interpretation of gravity anomalies to delineate some structural features of Biga and Gelibolu peninsulas, and their surroundings (north-west Turkey). *Geodin. Acta* **2015**, *27*, 300–319. [CrossRef]
77. Işık, E.; Büyüksaraç, A.; Ekinci, Y.L.; Aydın, M.C.; Harirchian, E. The effect of site-specific design spectrum on earthquake-building parameters: A case study from the Marmara Region (NW Turkey). *Appl. Sci.* **2020**, *10*, 7247. [CrossRef]
78. Anonymous. Historical Earthquakes. 2021. Available online: <https://deprem.afad.gov.tr> (accessed on 15 May 2022).
79. Anonymous. Historical Earthquakes. 2021. Available online: <http://www.koeri.boun.edu.tr> (accessed on 15 May 2022).
80. Ekinci, R.; Büyüksaraç, A.; Ekinci, Y.L.; Işık, E. Bitlis ilinin doğal afet çeşitliliğinin değerlendirilmesi. *Doğal Afetler Ve Çevre Derg.* **2020**, *6*, 1–11.
81. Özmen, B. Türkiye deprem bölgeleri haritalarının tarihsel gelişimi. *Türkiye Jeol. Bülteni* **2012**, *55*, 43–55.
82. Işık, E.; Ekinci, Y.L.; Sayıl, N.; Büyüksaraç, A.; Aydın, M.C. Time-dependent model for earthquake occurrence and effects of design spectra on structural performance: A case study from the North Anatolian Fault Zone, Turkey. *Turk. J. Earth Sci.* **2021**, *30*, 215–234. [CrossRef]
83. Pampal, S.; Özmen, B. Development of earthquake zoning maps of Turkey. In Proceedings of the Sixth National Conference on Earthquake Engineering, Istanbul, Turkey, 16–20 October 2007.
84. Işık, E. A comparative study on the structural performance of an RC building based on updated seismic design codes: Case of Turkey. *Challenge* **2021**, *7*, 123–134. [CrossRef]
85. Gülkan, P.; Koçyiğit, A.; Yüçemen, M.S.; Doyuran, V.; Başöz, N. *En son verilere göre hazırlanan Türkiye deprem bölgeleri haritası. Report No: METU/EERC, 93-101*; Department of Civil Engineering, Middle East Technical University: Ankara, Türkiye, 1993.
86. Aksoylu, C.; Arslan, M.H. 2007 ve 2019 deprem yönetmeliklerinde betonarme binalar için yer alan farklı deprem kuvveti hesaplama yöntemlerinin karşılaştırılması olarak irdelenmesi. *Int. J. Eng. Res. Dev.* **2021**, *13*, 359–374.
87. Nemutlu, Ö.F.; Balun, B.; Benli, A.; Sarı, A. Bingöl ve Elazığ illeri özelinde 2007 ve 2018 Türk deprem yönetmeliklerine göre ivme spektrumlarının değişiminin incelenmesi. *Dicle Üniversitesi Mühendislik Fakültesi Mühendislik Derg.* **2020**, *11*, 1341–1356.
88. AFAD. Available online: <https://www.afad.gov.tr/> (accessed on 18 May 2022).
89. Emre, Ö.; Duman, T.Y.; Özalp, S.; Şaroğlu, F.; Olgun, Ş.; Elmacı, H.; Çan, T. Active fault database of Turkey. *Bull. Earthq. Eng.* **2018**, *16*, 3229–3275. [CrossRef]
90. Kadirioğlu, F.T.; Kartal, R.F.; Kılıç, T.; Kalafat, D.; Duman, T.Y.; Azak, T.E.; Özalp, S.; Emre, Ö. An improved earthquake catalogue ( $M \geq 4.0$ ) for Turkey and its near vicinity (1900–2012). *Bull. Earthq. Eng.* **2018**, *16*, 3317–3338. [CrossRef]
91. Akkar, S.; Sandikkaya, M.A.; Bommer, J.J. Empirical ground-motion models for point-and extended-source crustal earthquake scenarios in Europe and the Middle East. *Bull. Earthq. Eng.* **2014**, *12*, 359–387. [CrossRef]
92. Moehle, J.; Deierlein, G.G. A framework methodology for performance-based earthquake engineering. In Proceedings of the 13th World Conference on Earthquake Engineering, Vancouver, BC, Canada, 1–6 August 2004; Volume 679.
93. Abrahamson, N.A.; Bommer, J.J. Probability and uncertainty in seismic hazard analysis. *Earthq. Spectra* **2005**, *21*, 603–607. [CrossRef]
94. Abrahamson, N.A.; Silva, W.J. Empirical response spectral attenuation relations for shallow crustal earthquakes. *Seismol. Res. Lett.* **1997**, *68*, 94–127. [CrossRef]
95. Campbell, K.W.; Bozorgnia, Y. Updated near-source ground-motion (attenuation) relations for the horizontal and vertical components of peak ground acceleration and acceleration response spectra. *Bull. Seismol. Soc. Am.* **2003**, *93*, 314–331. [CrossRef]
96. Graizer, V.; Kalkan, E. Ground motion attenuation model for peak horizontal acceleration from shallow crustal earthquakes. *Earthq. Spectra* **2007**, *23*, 585–613. [CrossRef]
97. Idriss, I.M. An NGA empirical model for estimating the horizontal spectral values generated by shallow crustal earthquakes. *Earthq. Spectra* **2008**, *24*, 217–242. [CrossRef]
98. Shafiq, A.; Ahmadi, H.R.; Bayat, M. Seismic investigation of cyclic pushover method for regular reinforced concrete bridge. *Struct. Eng. Mech.* **2021**, *78*, 41–52.
99. Antoniou, S.; Pinho, R. Advantages and limitations of adaptive and non-adaptive force-based pushover procedures. *J. Earthq. Eng.* **2004**, *8*, 497–522. [CrossRef]
100. Ferracuti, B.; Pinho, R.; Savoia, M.; Francia, R. Verification of displacement-based adaptive pushover through multi-ground motion incremental dynamic analyses. *Eng. Struct.* **2009**, *31*, 1789–1799. [CrossRef]
101. Pinho, R.; Casarotti, C.; Antoniou, S. A comparison of single-run pushover analysis techniques for seismic assessment of bridges. *Earthq. Eng. Struct. Dyn.* **2007**, *36*, 1347–1362. [CrossRef]

102. Casarotti, C.; Pinho, R. An adaptive capacity spectrum method for assessment of bridges subjected to earthquake action. *Bull. Earthq. Eng.* **2007**, *5*, 377–390. [[CrossRef](#)]
103. Seismosoft. SeismoStruct 2021—A Computer Program for Static and Dynamic Nonlinear Analysis of Framed Structures. 2021. Available online: <http://www.seismosoft.com> (accessed on 10 June 2022).
104. Antoniou, S.; Pinho, R. Development and verification of a displacement-based adaptive pushover procedure. *J. Earthq. Eng.* **2004**, *8*, 643–661. [[CrossRef](#)]
105. Navideh, M.; Hamid, R.A.; Hamed, M. A comparative study on conventional push-over analysis method and incremental dynamic analysis (IDA) approach. *Sci. Res. Essays* **2012**, *7*, 751–773. [[CrossRef](#)]
106. Pinho, R.; Antoniou, S. A displacement-based adaptive pushover algorithm for assessment of vertically irregular frames. In Proceedings of the Fourth European Workshop on the Seismic Behaviour of Irregular and Complex Structures, Thessaloniki, Greece, 26–27 August 2005.
107. Papanikolaou, V.K.; Elnashai, A.S. Evaluation of conventional and adaptive pushover analysis I: Methodology. *J. Earthq. Eng.* **2005**, *9*, 923–941. [[CrossRef](#)]
108. Caglar, N.; Demir, A.; Ozturk, H.; Akkaya, A. A simple formulation for effective flexural stiffness of circular reinforced concrete columns. *Eng. Appl. Artif. Intel.* **2015**, *38*, 79–87. [[CrossRef](#)]
109. Wilding, B.V.; Beyer, K. The effective stiffness of modern unreinforced masonry walls. *Earthq. Eng. Struct. Dyn.* **2018**, *47*, 1683–1705. [[CrossRef](#)]
110. Ugalde, D.; Lopez-Garcia, D.; Parra, P.F. Fragility-based analysis of the influence of effective stiffness of reinforced concrete members in shear wall buildings. *Bull. Earthq. Eng.* **2020**, *18*, 2061–2082. [[CrossRef](#)]